Colloid Polym Sci (2014) 292:333–342
DOI 10.1007/s00396-013-3072-0

ORIGINAL CONTRIBUTION

Magnetic and hydrophilic imprinted particles via ATRP at room temperature for selective separation of sulfamethazine

Yongli Zou · Chunyan Zhao · Jiangdong Dai · Zhiping Zhou · Jianming Pan · Ping Yu · Yongsheng Yan · Chunxiang Li

Received: 17 May 2013 / Revised: 7 September 2013 / Accepted: 7 September 2013 / Published online: 2 October 2013

Abstract In this work, a facile route to prepare hydrophilic molecularly imprinted particles with magnetic susceptibility (MMIPs) was first reported via atom transfer radical precipitation polymerization (ATRPP) in a methanol/water solvent at low temperature (298 K), which can be considered as an environment-friendly system. During the process, 2-hydroxyethyl methacrylate and *N*, *N*-methylenebisacrylamide monomers were added to improve the hydrophilicity of the polymers. The obtained materials were characterized in detail by X-ray diffraction, transform infrared spectroscopy, thermogravimetric analysis, vibrating sample magnetometer, scanning electron microscopy and transmission electron microscopy, and then used for the selective separation of sulfamethazine (SMZ) from aqueous medium. The images showed Fe_3O_4 nanoparticles that were successfully embedded into the polymer particles with the size ranging from 450 to 650 nm, which exhibited great superparamagnetic susceptivity and high thermal stability. Batch adsorption experiments were performed to determine specific adsorption equilibrium, kinetics, and selective recognition and separation. The effect of the ratio of the double monomers used in the adsorption property was also studied. The equilibrium data of MMIPs toward SMZ was well fitted by the Langmuir isotherm model, and the maximum adsorption capacity estimated was 66.67 μmol g^{-1}. The adsorption kinetics rapidly achieved equilibrium within 1.0 h and was well described by the pseudo-second-order model. The MMIPs synthesized showed outstanding affinity and selectivity toward SMZ over structurally analogous antibiotics and easily achieved magnetic separation under an external magnetic field. In addition, the adsorption performance of the resulting MMIPs was no obviously decreased at least six repeated cycles.

Keywords Magnetic and hydrophilic · Molecularly imprinted particles · ATRPP · Selective recognition and separation · Sulfamethazine

Y. Zou · C. Zhao · J. Pan · Y. Yan · C. Li (✉)
School of Chemistry and Chemical Engineering, Jiangsu University, Zhenjiang 212013, China
e-mail: zyl_1113@163.com

J. Dai · Z. Zhou
School of Material Science and Engineering, Jiangsu University, Zhenjiang 212013, China

Y. Zou · C. Zhao
School of the Environment and Safety Engineering, Jiangsu University, Zhenjiang 212013, China

P. Yu
School of Computer Science, Jilin Normal University, 1301 Haifeng Street, Siping 136000, China

Introduction

Molecularly imprinted technique allows the formation of tailor-made recognition sites in synthetic polymers through the use of the imprinted molecules [1]. The resultant molecularly imprinted polymers (MIPs) have shown not only high specificity and selectivity toward the template molecules but also excellent chemical, mechanical, and thermal stability, which make MIPs very promising candidates for many applications, such as catalysis [2, 3], chemical sensors [4, 5], solid phase extraction (SPE) [6, 7], separation techniques [8, 9] and so on. Up to now, one of the simplest methods available for MIPs preparation involves in conventional free radical bulk polymerization, which needs grind and sieve the monolith to a desired size range for the utilization [10]. Unfortunately, MIP particles with irregular size and shape are invariably obtained from grinding processes, which are wasteful (typically less than 50 % yield) and time-consuming. To simplify and optimize the preparation and performance of MIP particles,

alternative synthetic strategies have been developed to overcome the aforementioned drawbacks, including suspension [11], dispersion [12], and seeded polymerization [13]. While these methods have undoubted advantage, the general applicability is questionable, and residual emulsifier or stabilizer, which can interact with the monomer and template molecules, potentially compromises the binding strength and specificity [14]. Precipitation polymerization, as an alternative approach, is a surfactant-free method, which contributes to produce high-purity imprinted spherical particles [15].

Conventionally, free radical polymerization is the most popular technique to prepare MIPs [16]. However, the process is difficult to control over the size distribution, architecture, and number of synthesized macromolecules due to slow initiation, fast chain propagation, and termination reactions, as a result, which leads to broad binding site heterogeneity and relatively low affinity and selectivity [17]. In order to overcome these intrinsic limits, controlled/"living" radical polymerization (CRP) techniques have emerged in the past decade. Among, atom transfer radical polymerization (ATRP) [18], as a new technology, has been applied in generating MIPs [19, 20] because of various kinds of applicable monomers and the mild reaction conditions. Moreover, ATRP can be carried out in high polar solvents such as dimethylformamide, water, and methanol. To our best knowledge, except for some recent reports about MIPs prepared mostly by surface-initiated ATRP [21–24], there is no precedent for the preparation of MIPs by atom transfer radical precipitation polymerization (ATRPP) in an alcohol/water mixture, combining ATRP with precipitation polymerization, especially carried out at room temperature, which can be considered as an environmentally friendly system.

Magnetic nanoparticles have recently attracted significant interest because of unique properties and broad range of applications in many fields, such as magnetic separation, biosensor, and drug delivery [25]. If magnetic nanoparticles are functionalized with MIPs, magnetic MIPs (MMIPs) will have both magnetically susceptible characteristic and specific molecular recognition. Therefore, the MMIPs captured targets can be easily collected from sample solutions under an external magnetic field without additional centrifugation or filtration. MMIPs have been recently used to selectively recognize and remove targets from the complicated matrix [26, 27]. However, the strategy for preparing MMIPs by ATRPP has not been reported up to now.

Sulfonamides (SAs), as a group of antibacterial drugs, have been widely used in human therapy and farming industry for therapeutic, prophylactic, or growth promotion purposes because of the advantages of broad antibacterial spectrum, high efficacy, and low-cost [28]. The sulfonamides administered are poorly metabolized or absorbed by humans and animals, with being excreted unmetabolized via manure and consequently transporting into the aquatic environment, which do not strongly adhere to soil [29]. Exposures to residues of sulfonamides and their transformed products might cause allergy, carcinogenesis, and antibiotic resistance [30]. However, due to the extremely low concentration of residue, the removal of sulfonamides by conventional water treatment technologies is infeasible. Hence, the development of more effective and cheaper treatment technologies to remove sulfonamides from water is of great necessity. The separation of environmental contaminants from complicated matrices using MIPs has been recently demonstrated [31].

Herein, our work was the first attempt to prepare hydrophilic MMIPs using ATRPP in an alcohol/water mixture at room temperature and investigate the selective separation of MMIPs for SMZ from aqueous medium. The vinyl of γ-methacryloxypropyltrimethoxysilane (KH570) was introduced onto the surface of Fe_3O_4 nanoparticles using a coprecipitation method. In the process of imprinted polymerization, the obtained Fe_3O_4/KH570 nanoparticles were employed as magnetically susceptible copolymer substance, SMZ as template molecule, 4-vinylpyridine (4-VP), and 2-hydroxyethyl methacrylate (HEMA) as functional monomers, ethylene glycol dimethacrylate (EGDMA), and *N*,*N*-methylenebisacrylamide (MBAA) as cross-linker. Among, HEMA and MBAA were utilized to increase the hydrophilicity of the imprinted materials, enhancing the specific binding property in the pure water. The obtained materials were characterized by fourier transform infrared spectroscopy (FT-IR), X-ray diffraction (XRD), scanning electron microscopy (SEM), transmission electron microscopy (TEM), thermogravimetric analysis (TGA), and vibrating sample magnetometer (VSM). Most importantly, the special adsorption, adsorption kinetics, and selective recognition capacities of MMIPs were also investigated in detail.

Experimental section

Materials

Aqueous ammonia ($NH_3 \cdot H_2O$, 28 wt%), acetic acid, anhydrous toluene (99.8 %), methanol, copper (I) bromide (CuBr, 98 %), ferrous (II) sulfate heptahydrate ($FeSO_4 \cdot 7H_2O$, 99 %), and Iron (III) chloride hexahydrate ($FeCl_3 \cdot 6H_2O$, 99 %) were all analytical grade and obtained from Sinopharm Chemical Reagent Co., Ltd. (Shanghai, China). Ninety-six percent 4-VP, KH570 (98 %), HEMA (98 %), SMZ, tetracycline (TC, 98 %), chloroamphenicol (CAP, 98 %), ethyl α-bromoisobutyrate (EBiB, 98 %), *N*,*N*,*N*′,*N*′,*N*″-pentamethyl diethyenetriamine (PMDETA, 98 %), and MBAA (97 %) were purchased from Aladdin Reagent Co., Ltd. (Shanghai, China) and used as received. EGDMA (Aladdin Reagent Co. Ltd., Shanghai, China) was washed consecutively with 10 % aqueous NaOH, water and brine, dried over CaH_2, filtered,

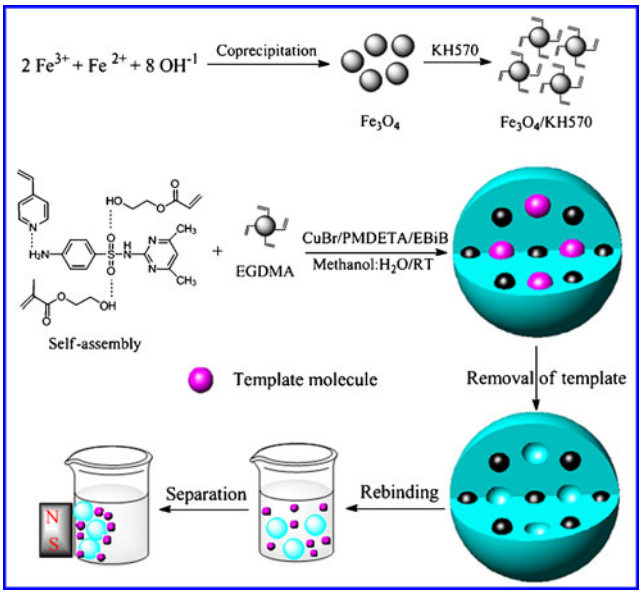

Fig. 1 Scheme of the synthesis route of MMIPs and magnetic separation

and then distilled under reduced pressure. Deionized ultrapure water was purified with a Purelab ultra (Organo, Tokyo, Japan).

Instruments

Infrared spectra were recorded on a Nicolet NEXUS-470 spectrophotometer using KBr pellets (USA). The identification of the crystallographic structure was performed using a Rigaku D/max-γB X-ray Diffractometer (XRD) with monochromatized with Cu Kα radiation over the 2θ range of 20–80° at a scanning rate of 0.02 deg s^{-1}. The morphology was observed by TEM (JEOL IEM-200CX) and field-emission scanning electron microscope (FE-SEM; S-4800). The measurements of magnetic particles were carried out using a VSM (HH-15, China) under a magnetic field up to 10 kOe. The TGA of samples was measured using a Diamond TG/DTA instruments (STA 449C Jupiter, Netzsch, Germany) under argon up to 800 °C with a heating rate of 10 °C min^{-1}.

Synthesis and modification of magnetic nanoparticles

Magnetic nanoparticles were prepared using a simple chemical coprecipitation. Typically, 0.04 mol of $FeCl_3 \cdot 6H_2O$ and 0.02 mol of $FeSO_4 \cdot 7H_2O$ were dissolved in 150 mL of distilled water in a three-necked bottom and heated to 80 °C under nitrogen. Subsequently, 20 mL of concentrated aqueous ammonia (28 wt%) was rapidly added into the solution. The mixture was vigorously stirred at 80 °C for 2.0 h. After cooling to room temperature, the obtained products were subjected to magnetic separation with a magnet, washed with ethanol and water several times, and were dried under vacuum.

KH570 (2.0 mL) and 1.0 g of the obtained Fe_3O_4 nanoparticles were dispersed into 100 mL of dry toluene and vigorously stirred under nitrogen at 110 °C for 12 h. The products were then collected and washed with toluene for several times. Finally, the modified magnetic particles (named Fe_3O_4/ KH570) were dried under vacuum.

Preparation of magnetic molecularly imprinted particles

Magnetic molecularly imprinted particles were prepared via ATRPP according to the following procedure: Briefly, Fe_3O_4/ KH570 (50 mg), HEMA (1.0 mmol), 4-VP (1.0 mmol), EGDMA (8.0 mmol), MBAA (0.8 mmol), and SMZ (0.5 mmol) were added in a mixture of methanol and water (3:1, *v*/*v*, 30 mL) in a one-neck round-bottom flask for prepolymerization at room temperature. The flask was

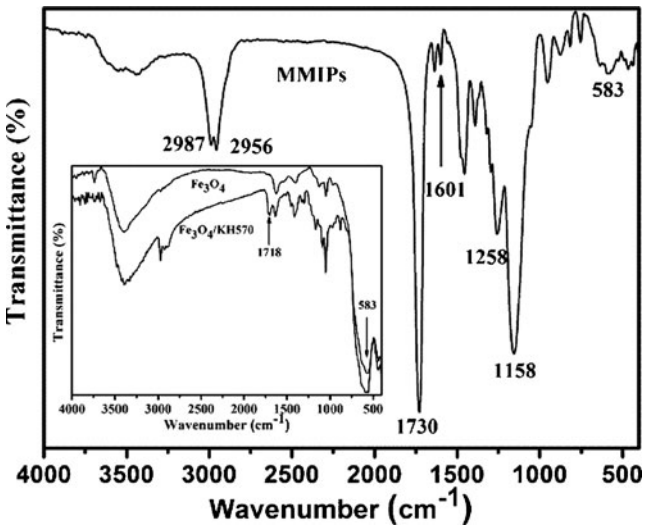

Fig. 2 FT-IR spectra of Fe_3O_4, Fe_3O_4/KH570 (inset), and MMIPs

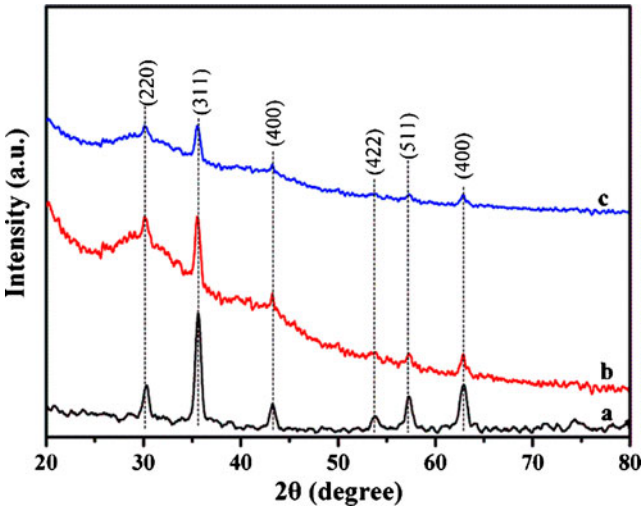

Fig. 3 X-ray diffraction pattern of Fe_3O_4 (*A*), Fe_3O_4/KH570 (*B*) nanoparticles, and MMIPs (*C*)

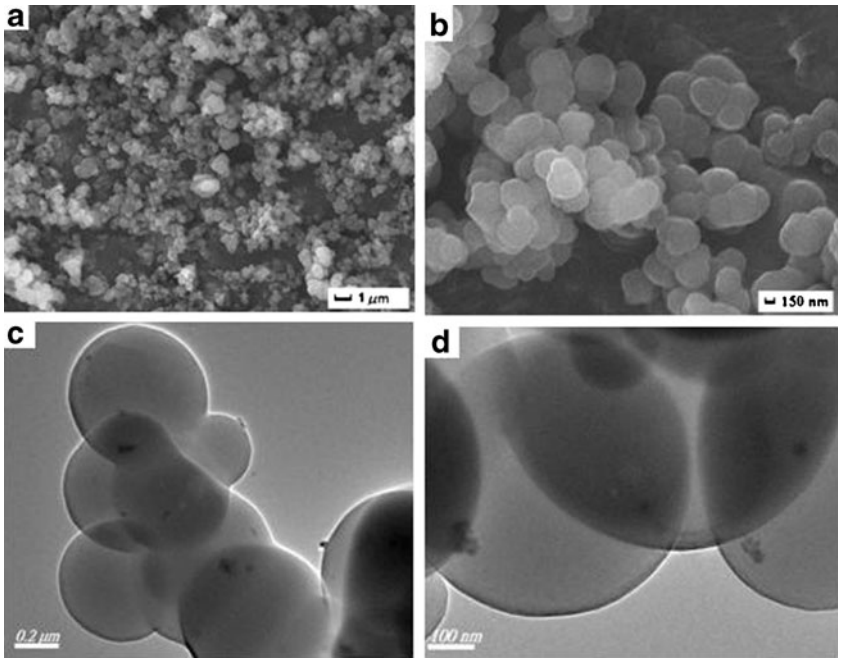

Fig. 4 SEM images (**a**, **b**) and TEM images (**c**, **d**) of MMIPs at different magnification

deoxygenated for 30 min by exchanging with nitrogen. Then CuBr (0.1 mmol) and PMDETA (0.15 mmol) were quickly transferred into the flask under the protection of nitrogen. Finally, the N_2-purged initiator EBiB (0.15 mmol) was injected into the reaction system. The reaction was allowed to proceed for 12 h at room temperature and then opened to air in order to stop polymerization. The products were collected by magnetic separation and washed thoroughly with water, ethanol, and acetone to remove the unreacted monomers. Then the materials were eluted in a Soxhlet apparatus with a mixture of methanol/acetic acid (9.0:1.0, *v*/*v*) until no SMZ could be detected by UV–vis (at 240 nm) in the eluent. The obtained MMIPs were then dried under vacuum for 12 h before use.

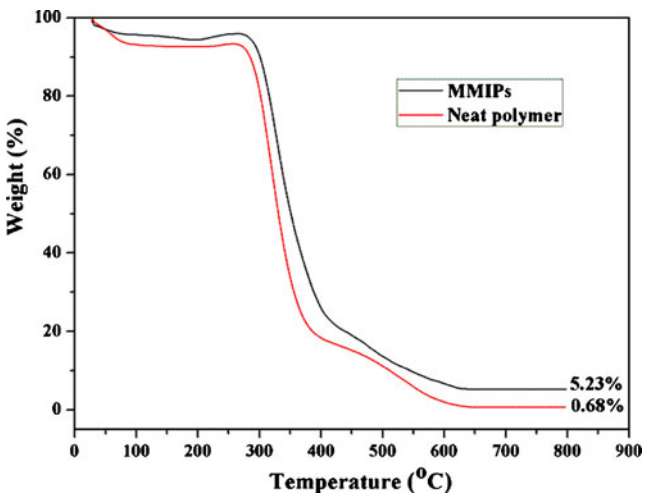

Fig. 5 Thermogravimetric analysis of the neat polymer and MMIPs

Correspondingly, the magnetic nonmolecularly imprinted particles (MNIPs) were prepared under the same procedure in the absence of template molecules.

Batch adsorption experiments

To study the adsorption equilibrium of the imprinted materials, 5.0 mg of MMIPs was added into 10 mL of SMZ solutions with initial concentrations ranging from 5.0 to 200 μmol L^{-1}. After 12 h, the saturated polymers were separated with an external magnet. The concentration of free SMZ in the supernate was determined by UV–vis at 249 nm. The equilibrium adsorption amounts of SMZ were calculated as follows:

$$Q_e = \frac{(C_o - C_e)V}{m} \quad (1)$$

where Q_e (μmol g^{-1}) is the amount of SMZ adsorbed at equilibrium, C_o and C_e (μmol L^{-1}) are the initial and equilibrium concentration, respectively. V is the volume, and m is the weight of adsorbents.

Similarly, the adsorption kinetics studies of MMIPs were performed by detecting the free SMZ concentration in the supernate at predetermined time intervals with the initial concentration of 100 μmol L^{-1}. The amount of SMZ adsorbed (Q_t, μmol g^{-1}) was calculated as follows:

$$Q_t = \frac{V(C_o - C_t)}{m} \quad (2)$$

where C_t (μmol L^{-1}) is the concentration of free SMZ solution at any time t (min).

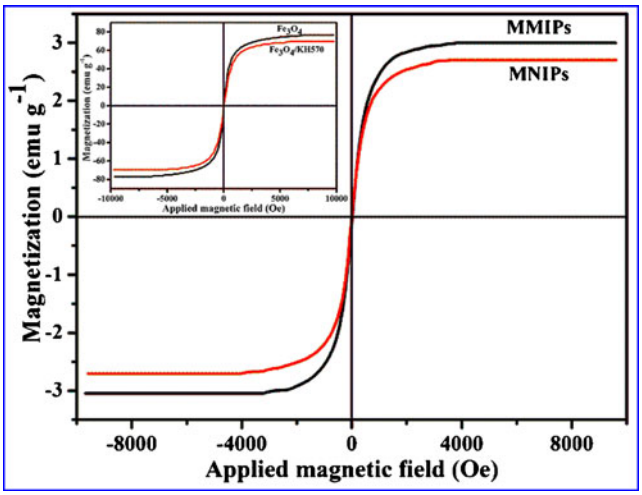

Fig. 6 Magnetization curves of bare Fe_3O_4, Fe_3O_4/KH570, MMIPs, and MNIPs

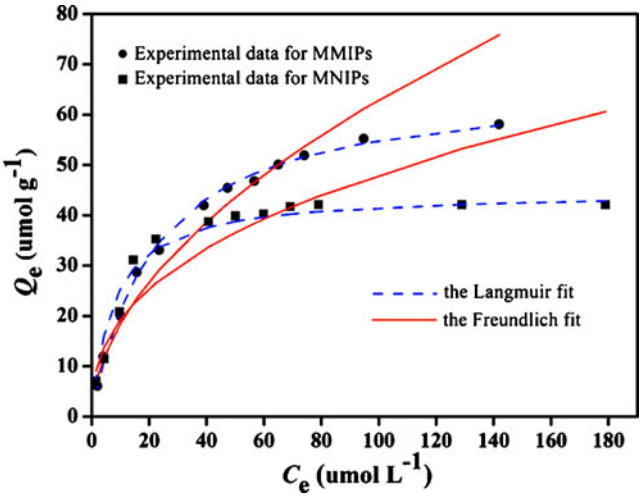

Fig. 8 Adsorption isotherms of MMIPs and MNIPs to SMZ with the fitting to the Langmuir and Freundlich model

To study the capacity of selectivity for MMIPs, 5.0 mg of MMIPs were added into test tubes containing 10 mL of sample solution with 100 μmol L^{-1} of SMZ, TC, and CAP, respectively. The initial solution pH was not adjusted, and the experiments were carried out at 25 °C for 12 h.

For comparison, the above experiments of MNIPs were performed under the same condition.

Results and discussion

Preparation of magnetic molecularly imprinted particles

Herein, we focused on the synthesis of the magnetic molecularly imprinted particles at room temperature, which was hydrophilic and easy to recognize and remove the SMZ from aqueous solution. Figure 1 illustrated the preparation route of MMIPs. Initially, the coprecipitation method was used to produce Fe_3O_4 nanoparticles, which presented narrow nanosize distribution and had a lot of hydroxyl group on the surface, following modification with KH570 via silanization reaction. The modification of magnetic nanoparticles was able to avoid oxidation and formation of aggregates due to the isolation from the air and the decrease of surface energy, respectively. Moreover, the vinyl monomers immobilized onto the surface of Fe_3O_4 nanoparticles could take part in the free radical polymerization.

Fig. 7 The profile of water contact angle of MMIPs (left); the photograph of the dispersion of MMIPs in the absence and in the presence of an external magnetic field (right)

In the subsequent process of imprinted polymerization, 4-VP and HEMA were chosen as functional monomer, considered that two monomers and SMZ could provide relatively strong hydrogen-binding interaction in the methanol/water (*v*/*v*, 3:1) mixture. The mole ratio of template molecule and monomer was 1: 4 in this work according to the research [32]. EGDMA and MBAA as cross-linking agent were chosen to participate in the polymerization. In order to increase the hydrophilicity of MMIPs, the HEMA and MBAA monomers were used to participate in the imprinted process. EBiB was employed as initiator, CuBr and PMDETA as catalysis system. The polymerization was started by the initiating radicals, which were produced via the reaction between an alkyl halide (EBiB) and a transition metal complex (Cu^+/PMDETA) in its lower oxidation state. The quick equilibrium between the active and dormant species was crucial to achieve controlled polymerization [33]. Here, ATRP was carried out in a methanol/water system (green and environmental-friendly) at room temperature in a relatively short time, which was efficient and well controlled, and has been extensively proved by the previous reports [34, 35].

Characterization of magnetic molecularly imprinted particles

The corresponding infrared absorption peaks can confirm the main functional groups of the predicted structures. Figure 2 showed the FT-IR spectroscopy measured of the bared Fe_3O_4,·Fe_3O_4/KH570 and MMIPs, respectively. A distinct absorption band at 583 cm^{-1} attributed to Fe–O bond in the

Table 1 Isotherm constants for SMZ adsorption onto MMIPs and MNIPs

Isotherm model		Langmuir			Freundlich			
Adsorbents	$Q_{e,\,exp}$ (μmol g^{-1})	Q_m (μmol g^{-1})	K_L (L μmol^{-1})	R^2	Q_m (μmol g^{-1})	K_F ((μmol g^{-1}) (L $\mu mol^{-1})^{1/n}$)	1/*n*	R^2
MMIPs	58.08	66.67	0.0463	0.9978	75.87	5.429	0.5322	0.9654
MNIPs	42.10	44.64	0.0132	0.9979	60.61	7.730	0.7037	0.9993

spectrum of Fe_3O_4 nanoparticles, which was also obtained for Fe_3O_4/KH570 and MMIPs. While, the strength of Fe–O stretching markedly decreased due to the coated thick polymers, which clearly confirmed the success of polymerization. Compared with the Fe_3O_4, the infrared spectroscopy of Fe_3O_4/KH570 displayed the characteristic peak of carbonyl group at 1,718 cm^{-1} marked by the arrow, which confirmed that KH570 were successfully grafted onto the surface of Fe_3O_4 nanoparticles via the silanization reaction [36]. A broad absorption band at 3,450 cm^{-1} of the MMIPs corresponded to the stretching vibration of the hydroxyl groups for HEMA molecules and the −NH groups of MBAA molecules. The C–O and C–N stretching vibration bands of ester (EGDMA and MBAA, respectively) were around 1,258 and 1,158 cm^{-1}, respectively [37]. The typical absorption bands of MMIPs were at 2,987 and 2,956 cm^{-1} assigned to the C–H asymmetry stretching vibrations of both $-CH_3$ and $-CH_2$ groups. The characteristic peaks corresponding to the C=N stretching (1,601 and 1,558 cm^{-1}) and C=C stretching (1,456 cm^{-1}) in the pyridine rings can also be observed in the spectra of MMIPs. The above results explained that the imprinted process using ATRPP was successfully achieved.

The X-ray power diffraction of the Fe_3O_4, Fe_3O_4/KH570, and MMIPs were shown in Fig. 3. In the 2θ region of 20–80°, six diffraction peaks were indexed as (220), (311), (400), (422), (511), (440), and (533), respectively (JCPDS card: 19–0629). Compared with the Fe_3O_4, the six peak positions of Fe_3O_4/KH570 and MMIPs were unchanged, indicating that the crystalline structure of the magnetite is essentially maintained. However, the peak intensity of Fe_3O_4/KH570 slightly decreased, confirming that KH570 was immobilized on the surface of Fe_3O_4 nanoparticles successfully. Furthermore, the obvious decrease of the peak intensity for MMIPs demonstrated that the Fe_3O_4/KH570 successfully participated in ATRPP and was coated by imprinted polymers.

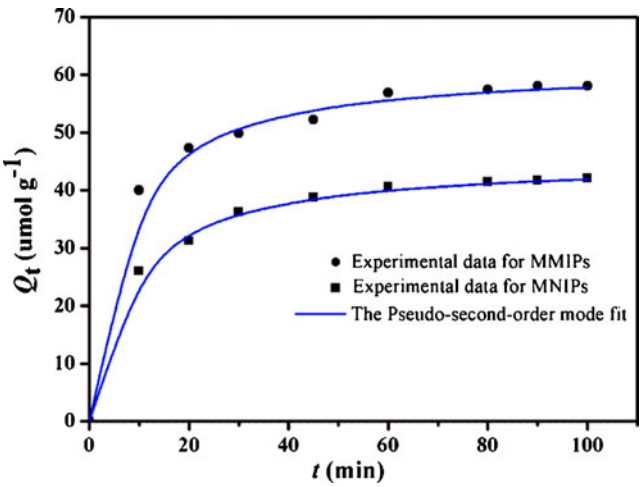

Fig. 9 Adsorption kinetic curves of MMIPs and MNIPs to SMZ with the fitting to the pseudo-second-order kinetic model

As shown in Fig. 4, SEM and TEM were used to capture the microscopic images of the MMIPs prepared. SEM images (shown in Fig. 4a, b) revealed that MMIPs were near-spherical particles with size ranging from 450 to 650 nm, which also could be observed in Fig. 4c, d. Fe_3O_4 nanoparticles with the mean size of around 10 nm were successfully encapsulated into the polymers, which shared magnetic susceptibility and resulted in the decrease of the saturation magnetization of the whole MMIPs matching with the results of the VSM.

The thermogravimetric analysis (TGA) was employed to further quantify the encapsulated amount of Fe_3O_4 and detect thermal stability of MMIPs. As can be seen in Fig. 5, TGA curves of MMIPs were composed of three stages of mass change between 25 and 800 °C. The first stage started from room temperature to 250 °C, the loss of weight was 4.78 %, which may caused by the dehydration. The loss of imprinted polymers led to significant mass loss in the second stage occurred from 250 to 450 °C, the value of which was 89.99 %. The mass remained relatively constant for the rest of the analysis up to 800 °C. The remnant was attributed to the more thermally resistant Fe_3O_4 nanoparticles and extremely little silica, and thus magnetite encapsulation efficiency of MMIPs was about 4.55 %, which was calculated by reducing the residual carbon content of neat polymer. The encapsulation efficiency was relatively high and satisfactory, which could be demonstrated by the magnetic separation experiment.

VSM analysis was applied to investigate magnetic property of Fe_3O_4, Fe_3O_4/KH570, MMIPs, and MNIPs. As can be seen in Fig. 6, the magnetization curves of four samples were no hysteresis and symmetrical about the origin, suggesting that samples were superparamagnetic, which made magnetic separation and reusability easy. The saturation magnetization

Table 2 Kinetics parameters for SMZ adsorption onto MMIPs and MNIPs

Kinetic model		Pseudo-first-order			Pseudo-second-order		
Adsorbents	$Q_{e,\,exp}$ (μmol g^{-1})	$Q_{e,\,c}$ (μmol g^{-1})	k_1 (min^{-1})	R^2	$Q_{e,\,c}$ (μmol g^{-1})	k_2 (g μmol^{-1} min^{-1})	R^2
MMIPs	58.08	32.58	0.0492	0.9039	61.35	0.0027	0.9993
MNIPs	42.10	23.53	0.0442	0.9894	45.05	0.0030	0.9996

(*Ms*) values of Fe_3O_4 and Fe_3O_4/KH570 at 298 K were 76.50 and 69.48 emu g^{-1} (shown in Fig. 6a), respectively. The decrease of *M*s also indicated that the vinyl was modified onto the surface of Fe_3O_4 nanoparticles. The *M*s of MMIPs and MNIPs were 3.04 and 2.70 emu g^{-1} (shown in Fig. 6b), respectively, which agreed with the results of TGA. The obvious decrease of *Ms* was expected because the polymer coating had effectively shielded the magnetite.

The result of the water contact angle for MMIPs was showed in Fig. 7, the value of which was 79.17° (<90°), indicating that the material was hydrophilic. The MMIPs were dispersed into the pure water to form a brown homogeneous system. When close to the external magnetic field, the brown particles were fast attracted to the wall of vial, and the solution simultaneously turned to be transparent, which illustrated that MMIPs was an ideal magnetic separation carrier.

Adsorption isotherms

To test the adsorption capacity and the equilibrium constants of the materials synthesized toward SMZ, the adsorption isotherm experiments were performed at different initial concentrations. Langmuir and Freundlich isotherm model were used to fit the experimental data. The nonlinear expression of the Langmuir [38] and Freundlich equation [39] were listed as Eqs. (3) and (4), respectively.

$$Q_e = \frac{K_L Q_m C_e}{1 + K_L C_e} \tag{3}$$

$$Q_e = K_F C_e^{1/n} \tag{4}$$

where Q_e (μmol g^{-1}) is the equilibrium amount of SMZ adsorbed, C_e (μmol L^{-1}) and Q_m (μmol g^{-1}) were the equilibrium concentration of SMZ and the maximum adsorption capacity, respectively. K_L (L μmol^{-1}) is the Langmuir constant, and K_F ((μmol g^{-1}) (L $\mu mol^{-1})^{1/n}$) is the Freundlich constant.

As seen in Fig. 8, compared with the MNIPs, MMIPs exhibited higher adsorption capacity in the whole concentration range. The adsorption capacity of MMIPs toward SMZ in aqueous solution was 58.08 μmol g^{-1} and much larger than that of the previous SMZ-MIPs by other researchers [40, 41], which were mostly prepared using the time-consuming bulk polymerization at high temperatures. Here, we adopted a simple and green route, the ATRPP method, for preparation of magnetic and hydrophilic imprinted polymer particles in the methanol/water mixture at room temperature. The regression curves of Langmuir and Freundlich isotherm models for MMIPs and MNIPs were obtained, respectively, and the involved parameters were shown in Table 1. The regression coefficient of Langmuir model was relatively higher (above 0.99) for both MMIPs and MNIPs, which illustrated that Langmuir isotherm fitted quite better with the experimental data than Langmuir isotherm. The maximum adsorption capacities calculated by Langmuir isotherm was 66.67 and 44.64 μmol g^{-1} for MMIPs and MNIPs, respectively, which was close to the experimental data. The results suggested that the active sites distribution of MMIPs and MNIPs was homogeneous owing to the nature of ATRPP.

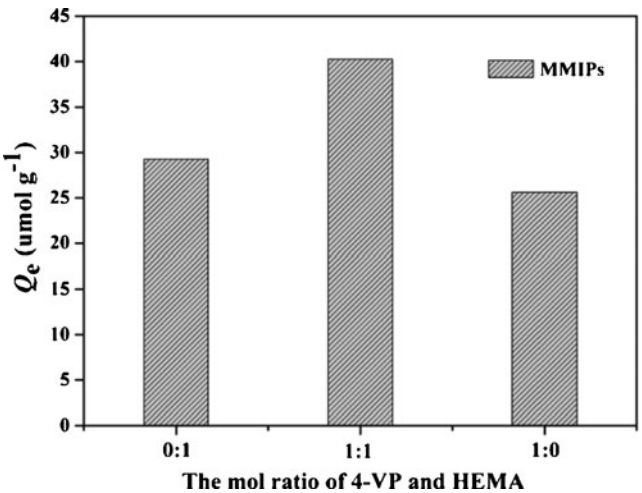

Fig. 10 Effect of functional monomers to adsorption capacity of MMIPs to SMZ molecules

Adsorption kinetics

Figure 9 showed the adsorption kinetic spots of SMZ adsorbed toward MMIPs and MNIPs with the initial concentration of 100 μmol L^{-1} at interval time. The rapid increase of adsorption amount was observed in the first 60 min, owing to

a large amount of empty and active cavities, which enabled templates to be easily entered. Subsequently, the equilibrium slowly achieved, once SMZ occupied most of cavities.

To study the mechanism of adsorption, the pseudo-first-order [42] and pseudo-second-order rate models [43] were used to fit the kinetic data obtained from the experiments. The two models can be listed as follows:

$$Q_t = Q_e - Q_e e^{-k_1 t} \quad (5)$$

$$Q_t = \frac{k_2 Q_e^2 t}{1 + k_2 Q_t t} \quad (6)$$

where Q_e (μmol g^{-1}) and Q_t (μmol g^{-1}) are the amount of SMZ adsorbed at equilibrium and at any time t, respectively. k_1 (min^{-1}) and k_2 (g μmol^{-1} min^{-1}) are the pseudo-first-order rate constant and the pseudo-second-order rate constant, respectively.

Figure 9 exhibited the nonlinear regression curve of the pseudo-second-order rate equation for SMZ adsorption onto MMIPs and MNIPs, and the kinetic constants of the two kinetic models were listed in Table 2. The low regression coefficients value (R^2) and large variance between the experimental and theoretical values indicated that the pseudo-first-order model was unfavorable. The favorable agreement between experimental and fitted values of Q_e (R^2 values above 0.99) indicated that the adsorption of MMIPs toward SMZ obeyed the pseudo-second-order model well and chemical adsorption may be the rate-limiting step, which was predominant in the recognition process [44].

Effect of functional monomer

In order to investigate the effect of hydrophilicity of MMIPs in the recognition of SMZ, different functional monomers were used in the process of polymerization, which resulted in the difference of adsorption capacity observed in Fig. 10. As can been seen, when the functional monomers comprised 4-VP and HEMA (mol/mol, 1:1), the value of adsorption amount for SMZ was 40.23 μmol g^{-1}, with the initial concentration of 80 μmol L^{-1}, which was larger than that in present of a single functional monomer. The MMIPs using 4-VP as the sole monomer exhibited better adsorption performance than in the existence of HEMA due to the stronger interaction between SMZ and 4-VP. The results demonstrated that double-functional monomers were favorable for the imprinted process via ATRPP in an aqueous system.

Selectivity property of MMIPs

To investigate the selectivity of the prepared MMIPs toward SMZ molecules, TC and CAP were chosen as reference antibiotics with different molecule structures. The batch

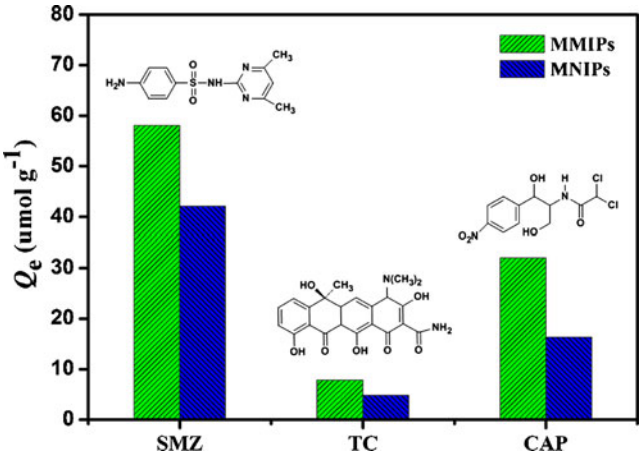

Fig. 11 Adsorption capacity of MMIPs and MNIPs to template SMZ and other two antibiotics

adsorption experiments were carried out at 298 K with an initial concentration of 100 μmol L^{-1}, and the adsorption capacities of MMIPs and MNIPs for the three antibiotics were determined, which was shown in Fig. 10. Compared with TC and CAP, the MMIPs exhibited high adsorption capacity for SMZ, indicating the obtained imprinted materials had great selective recognition of template molecules. The adsorption amount of MMIPs toward TC was only 7.83 μmol g^{-1} because the structure of TC was larger than the imprinted cavity left by the elution of SMZ. CAP molecules may enter the active sites, the hydroxyl, amine, and nitro groups of which can interact with the functional monomers. Therefore, the adsorption amount of MMIPs toward CAP was relatively large. Figure 11 also clearly illustrated that the adsorption amount of MMIPs toward the three antibiotics was larger than that of MNIPs. The process of the selective recognition was always considerably complicated; besides the hydrogen interaction and structural selectivity, others interactions may also be involved, such as electrostatic attraction and hydrophobic interaction.

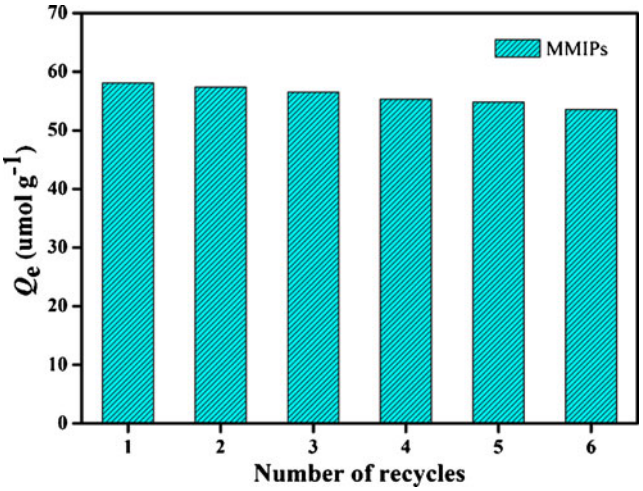

Fig. 12 Recycle and stability of MMIPs to SMZ

Recycle of MMIPs

Six regeneration cycles were performed under the same condition, in order to verify the stability and recycle the MMIPs. Typically, 5.0 mg of MMIPs was added into 10 mL of 100 μmol L^{-1} SMZ solution. After the supernatant solution was discarded with the help of magnetic separation, the MMIPs were dipped in 10 mL of eluent under the ultrasound, which composed of methanol and acetic acid (9.0:1.0, *v*/*v*). Figure 12 showed the each result of adsorption of MMIPs toward SMZ. After six recycles, the loss of adsorption mount for MMIPs toward SMZ was around 7.18 %, suggesting great stability of the imprinted materials.

Conclusions

In conclusion, we successfully synthesized magnetic and hydrophilic molecularly imprinted particles using atom transfer radical precipitation polymerization in a methanol/water mixture, which was green and environment-friendly. Owing to the technique, MMIPs can be prepared at a low temperature (298 K). The detailed characterization indicated Fe_3O_4 nanoparticles modified by KH570 were successfully embedded into imprinted polymers and MMIPs exhibited thermal stability and magnetic susceptivity, which enhanced the desired efficiency of fast separation. The results of batch adsorption experiments demonstrated that MMIPs had good performance such as excellent adsorption capacity, selective recognition, and fast adsorption kinetics. The utilization of HEMA and MBAA monomers improved the hydrophilicity of MMIPs, which was in favor of specific recognition and separation of SMZ from aqueous mediums. The MMIPs also exhibited excellent property of regeneration and stability. From all the results, the imprinted polymer materials have great potential in the selective separation of environment pollutions.

Acknowledgments This work was financially supported by the National Natural Science Foundation of China (nos. 21077046, 21004031, 21176107, and 21174057), the National Basic Research Program of China (973 Program, 2012CB821500), Ph.D. Programs Foundation of Ministry of Education of China (no. 20110205110014), and Natural Science Foundation of Jiangsu Province (BK2011461).

References

1. Wulff G (2002) Enzyme-like catalysis by molecularly imprinted polymers. Chem Rev 102:1–27
2. Chen ZY, Xu L, Liang Y, Zhao MP (2010) PH-Sensitive water-soluble nanospheric imprinted hydrogels prepared as horseradish peroxidase mimetic enzymes. Adv Mater 22:1488–1492
3. Shen XT, Zhu LH, Li J, Tang HQ (2007) Synthesis of molecular imprinted polymer coated photocatalysts with high selectivity. Chem Commun 11:1163–1165
4. Matsui J, Sodeyama T, Saiki Y, Miyazawa T, Yamada T, Tamaki K, Murashima T (2009) Face-to-face porphyrin moieties assembled with spacing for pyrazine recognition in molecularly imprinted polymers. Biosens Bioelectron 25:635–639
5. Basabe-Desmonts L, Reinhoudt DN, Crego-Calama M (2007) Design of fluorescent materials for chemical sensing. Chem Soc Rev 36: 993–1017
6. Mullett WM, Martin P, Pawliszyn J (2001) In-tube molecularly imprinted polymer solid-phase microextraction for the selective determination of propranolol. Anal Chem 73:2383–2389
7. Ariffin MM, Miller EI, Cormack PAG, Anderson RA (2007) Molecularly imprinted solid-phase extraction of diazepam and its metabolites from hair samples. Anal Chem 79:256–262
8. Yin JF, Yang GL, Chen Y (2005) Rapid and efficient chiral separation of nateglinide and its l-enantiomer on monolithic molecularly imprinted polymers. J Chromatogr A 1090:68–75
9. Zhang W, Qin L, He XW, Li WY, Zhang YK (2009) Novel surface modified molecularly imprinted polymer using acryloyl-β-cyclodextrin and acrylamide as monomers for selective recognition of lysozyme in aqueous solution. J Chromatogr A 1216: 4560–4567
10. Beltran A, Borrull F, Marcé RM, Cormack PAG (2010) Molecularly-imprinted polymers: useful sorbents for selective extractions. TrAC Trends Anal Chem 29:1363–1375
11. Tamayo FG, Turiel E, Martín-Esteban A (2007) Molecularly imprinted polymers for solid-phase extraction and solid-phase microextraction: recent developments and future trends. J Chromatogr A 1152:32–40
12. Sellergren B (1994) Direct drug determination by selective sample enrichment on an imprinted polymer. Anal Chem 66:1578–1582
13. Pérez-Moral N, Mayes AG (2004) Comparative study of imprinted polymer particles prepared by different polymerization methods. Anal Chim Acta 504:15–21
14. Ye L, Mosbach K (2001) Molecularly imprinted microspheres as antibody binding mimics. React Funct Polym 48:149–157
15. Wang JF, Cormack PAG, Sherrington DC, Khoshdel E (2003) Monodisperse molecularly imprinted polymer microspheres prepared by precipitation polymerization for affinity separation applications. Angew Chem Int Ed 42:5336–5338
16. Chen LX, Xu SF, Li JH (2011) Recent advances in molecular imprinted technology: current status, challenges and highlighted applications. Chem Soc Rev 40:2922–2942
17. Zu BY, Pan GQ, Guo XZ, Zhang Y, Zhang HQ (2009) Preparation of molecularly imprinted polymer microspheres via atom transfer radical precipitation polymerization. J Polym Sci Part A Polym Chem 47: 3257–3270
18. Matyjaszewski K, Xia J (2001) Atom transfer radical polymerization. Chem Rev 101:2921–2990
19. Zu BY, Pan GQ, Guo XZ, Zhang Y, Zhang HQ (2010) Preparation of molecularly imprinted polymers via atom transfer radical "bulk" polymerization. J Polym Sci Part A Polym Chem 48:532–541
20. Sasaki S, Ooya T, Takeuchi T (2010) Highly selective bisphenol A-imprinted polymers prepared by atom transfer radical polymerization. Polym Chem 1:1684–1688
21. Gai QQ, Qua F, Zhang T, Zhang YK (2011) The preparation of bovine serum albumin surface-imprinted superparamagnetic polymer with the assistance of basic functional monomer and its application for protein separation. J Chromatogr A 1218:3489–3495
22. Wei X, Husson SM (2005) Surface molecular imprinting by atom transfer radical polymerization. Biomacromolecules 6:1113–1121
23. Lu CH, Wang Y, Li Y, Yang HH, Chen X, Wang XR (2009) Bifunctional superparamagnetic surface molecularly imprinted polymer core-shell nanoparticles. J Mater Chem 19:1077–1079

24. Wei X, Husson SM (2007) Surface-grafted molecularly imprinted polymers grown from silica gel for chromatographic separations. Ind Eng Chem Res 46:2117–2124
25. Laurent S, Forge D, Port M, Roch A, Robic C, Elst LV, Muller RN (2008) Magnetic iron oxide nanoparticles: synthesis, stabilization, vectorization, physicochemical characterizations, and biological applications. Chem Rev 108:2064–2110
26. Arteaga KA, Rodriguez JA, Miranda JM, Medina J, Barrado E (2010) Determination of non-steroidal anti-inflammatory drugs in wastewaters by magnetic matrix solid phase dispersion-HPLC. Talanta 80:1152–1157
27. Zhang Y, Liu RJ, Hu YL, Li GK (2009) Microwave heating in preparation of magnetic molecularly imprinted polymer beads for trace triazines analysis in complicated samples. Anal Chem 81:967–976
28. Sarmah AK, Meyer MT, Boxall ABA (2006) A global perspective on the use, sales, exposure pathways, occurrence, fate and effects of veterinary antibiotics (VAs) in the environment. Chemosphere 65: 725–759
29. Halling-Sørensen B, Nors-Nielsen S, Lanzky PF, Ingerslev F, Holten-Lützhøft HC, Jørgensen SE (1998) Occurrence, fate, and effects of pharmaceutical substances in the environment a review. Chemosphere 36:357–393
30. Martinez JL (2008) Antibiotics and antibiotic resistance genes in natural environments. Science 321:365–367
31. Hu YL, Li YW, Liu RJ, Tan W, Li GK (2011) Magnetic molecularly imprinted polymer beads prepared by microwave heating for selective enrichment of β-agonists in pork and pig liver samples. Talanta 84:462–470
32. Zheng N, Li YZ, Chang WB, Wang ZM, Li TJ (2002) Sulfonamide imprinted polymers using co-functional monomers. Anal Chim Acta 452:277–283
33. Matyjaszewski K (1999) Copper (I)-catalyzed atom transfer radical polymerization. Acc Chem Res 32:895–903
34. Robinson KL, Khan MA, de Paz Báñez MV, Wang XS, Armes SP (2001) Controlled polymerization of 2-hydroxyethyl methacrylate by aTRP at ambient temperature. Macromolecules 34:3155–3158
35. Wan WM, Pan CY (2007) Atom transfer radical dispersion polymerization in an ethanol/water mixture. Macromolecules 40:8897–8905
36. Du BY, Mei AX, Tao PJ, Zhao B, Cao Z, Nie JJ (2009) Poly[N-isopropylacrylaminde-co −3(trimethoxysilyl)-propylmethacrylate] coated aqueous dispersed thermosensitive Fe_3O_4 nanoparticle. J Phys Chem C 113:10090–10096
37. Yoshimatsu K, Reimhult K, Krozer A, Mosbach K, Sode K, Ye L (2007) Uniform molecularly imprinted microspheres and nanoparticles prepared by precipitation polymerization: the control of particle size suitable for different analytical applications. Anal Chim Acta 584:112–121
38. Langmuir I (1918) The adsorption of gases on plane surfaces of glass, mica and platinum. J Am Chem Soc 40:1361–1403
39. Umpleby RJ II, Baxter SC, Rampey AM, Rushton GT, Chen Y, Shimizu KD (2004) Characterization of the heterogeneous binding site affinity distributions in molecularly imprinted polymers. J Chromatogr B 804:141–149
40. Valtchev M, Palm BS, Schiller M, Steinfeld U (2009) Development of sulfamethoxazole-imprinted polymers for the selective extraction from waters. J Hazard Mater 170:722–728
41. Shi XZ, Meng Y, Liu JH, Sun AL, Li DX, Yao CX, Lu Y, Chen J (2011) Group-selective molecularly imprinted polymer solid-phase extraction for the simultaneous determination of six sulfonamides in aquaculture products. Journal of Chromatography B 879:1071–1076
42. Ho YS, McKay G (1999) The sorption of lead (II) ions on peat. Water Res 33:578–584
43. Ho YS, McKay G (1999) Pseudo-second order model for sorption processes. Process Biochem 34:451–465
44. Baydemir G, Andac M, Bereli N, Say R, Denizli A (2007) Selective removal of bilirubin from human plasma with bilirubin-imprinted particles. Ind Eng Chem Res 46:2843–2852